Developmental Cognitive Neuroscience 31 (2018) 20–34

Contents lists available at ScienceDirect

Developmental Cognitive Neuroscience

journal homepage: www.elsevier.com/locate/dcn

Neural substrates of the influence of emotional cues on cognitive control in risk-taking adolescents

Nikki C. Lee[a,b,*,1], Wouter D. Weeda[c,1], Catherine Insel[d], Leah H. Somerville[d], Lydia Krabbendam[a], Mariëtte Huizinga[b]

[a] Department of Clinical, Neuro- and Developmental Psychology, Faculty of Behavioural and Movement Sciences, Vrije Universiteit Amsterdam, The Netherlands
[b] Department of Education and Family Studies, Faculty of Behavioural and Movement Sciences, Vrije Universiteit Amsterdam, The Netherlands
[c] Department of Psychology, Faculty of Social and Behavioural Sciences, Leiden University, The Netherlands
[d] Department of Psychology and Center for Brain Science, Harvard University, USA

ARTICLE INFO

Keywords:
Adolescence
Risk-taking
Cognitive control
Emotion
fMRI
Inferior frontal gyrus
Dorsal striatum

ABSTRACT

Adolescence is a period characterised by increases in risk-taking. This behaviour has been associated with an imbalance in the integration of the networks involved in cognitive control and motivational processes. We examined whether the influence of emotional cues on cognitive control differs between adolescents who show high or low levels of risk-taking behaviour. Participants who scored especially high or low on a risky decision task were subsequently administered an emotional go/no-go fMRI task comprising angry, happy and calm faces. Both groups showed decreased cognitive control when confronted with appetitive and aversive emotional cues. Activation in the inferior frontal gyrus (IFG) increased in line with the cognitive control demands of the task. Though the risk taking groups did not differ in their behavioural performance, functional connectivity analyses revealed the dorsal striatum plays a more central role in the processing of cognitive control in high than low risk-takers. Overall, these findings suggest that variance in fronto-striatal circuitry may underlie individual differences in risk-taking behaviour.

1. Introduction

Adolescence is a period characterised by increases in risk-taking and reward seeking, behaviours which have been described as both adaptive and maladaptive (Galvan, 2013). Though these tendencies have often been related to adverse outcomes, such as increases in instances of unintentional injuries, road traffic accidents, unsafe sexual behaviour and substance abuse (Eaton et al., 2012; Geier, 2013), recent work has also suggested that higher levels of risk-taking may lead to increased exploration-based learning (Humphreys et al., 2013; Silva et al., 2016). Adolescents appear to respond differently to risks than adults, and both the positive and negative consequences of the resulting risk-taking behaviours suggest that an increased understanding of the mechanisms underlying this behaviour could have important societal implications.

At a neural level, various models have been proposed to explain adolescent risk-taking. A set of so-called dual systems or imbalance models has suggested that this behaviour is associated with a disparity in the integration of the networks involved in motivational processes and inhibitory control (for recent overviews see Casey et al., 2016; Crone and Dahl, 2012; Schulman et al., 2016). These models posit that adolescence, compared to childhood and adulthood, is characterised by changes in activity in subcortical circuitry involved in affect and reward processing, such as the amygdala and ventral striatum (Galvan et al., 2006; Somerville et al., 2011). Conversely, the prefrontal cognitive control systems which interact with motivational systems show a more linear and protracted development. With age, frontal control over subcortical regions is thought to increase, thereby enabling greater behavioural regulation (Heller et al., 2016; Vink et al., 2014). But during adolescence these cortico-subcortical circuits are still developing, leading to a developmental imbalance in the influence of subcortical systems on behaviour (Casey et al., 2016; Mills et al., 2014). Consequently, when adolescents are exposed to emotionally or motivationally salient information they are often unable to sufficiently recruit inhibitory control resources to down-regulate robust appetitive drives. This leads to a greater influence of appetitive information on adolescent behaviour than during childhood and adulthood, often resulting in impulsive behaviour.

While there is much research that supports these imbalance models,

* Corresponding author at: Department of Clinical, Neuro- and Developmental Psychology, Section of Clinical Developmental Psychology, Faculty of Behavioural and Movement Sciences, Vrije Universiteit Amsterdam, Van der Boechorststraat 1, 1081 BT Amsterdam, The Netherlands.
E-mail address: n.c.lee@vu.nl (N.C. Lee).
[1] These authors Contributed equally to this work.

https://doi.org/10.1016/j.dcn.2018.04.007
Received 16 February 2017; Received in revised form 26 March 2018; Accepted 18 April 2018
Available online 22 April 2018

some have suggested that the claims may be overly simplistic, and do not fully reflect the diversity of findings within the field (see for example Pfeifer and Allen, 2012). For example, while numerous studies have shown hyperresponsiveness in the amygdala and striatum during adolescence (e.g. Chein et al., 2011; Guyer et al., 2008; Hare et al., 2008; Somerville et al., 2011), there are also a number of studies which did not replicate these findings (e.g. Bjork et al., 2010; Geier et al., 2010; see also Scherf et al., 2013). This has led to the suggestion that adolescent neural responses may vary as a function of stimuli, context and task demands (Nelson et al., 2016). For example, in situations where motivational and affective demands are low, adolescents are often able to exhibit regulatory function that is comparable to that of adults (Crone and Dahl, 2012). However, the reality of adolescence is that many of the situations adolescents find themselves in are emotionally charged, for example due to the presence of their peers. During adolescence social relationships become increasingly important, and consequently social acceptance becomes a powerful motivator for adolescents to conform to patterns of behaviour that receive approval from their social group (Allen et al., 2005). As a result, they are frequently confronted with situations with could potentially undermine their developing cognitive control abilities, and some are able to navigate this more successfully than others. The current study aims to elucidate how the interplay between emotional cues and cognitive control differs between adolescents who show high or low levels of risk-taking behaviour.

A number of previous studies have assessed the interaction between emotional cues and inhibitory control using an emotional go/no-go paradigm, though these interactions have not been explicitly linked to risk-taking behaviours. Compared to adults and children, adolescents appear to be less able to suppress responses to appetitive cues such as happy faces, as well as showing enhanced reward-related activation in the ventral striatum in response to these stimuli (Somerville et al., 2011). Aversive stimuli, such as fearful or threatening faces, similarly decrease inhibitory control and slow response times in adolescent samples (Cohen-Gilbert and Thomas, 2013). These behaviours are paralleled by increased activation during the task in limbic regions such as the amygdala, and decreased recruitment of prefrontal regions, rendering adolescents more sensitive to emotional interference during the task (Dreyfuss et al., 2014; Hare et al., 2008). Increased connectivity between these regions has been associated with improvements in cognitive control (Heller et al., 2016). Even in a task where the emotional information was task-irrelevant, adolescents were more distracted than adults by negative stimuli, though not by positive stimuli (Cohen-Gilbert and Thomas, 2013; Grose-Fifer et al., 2013). These studies suggest that adolescents find it more difficult than children or adults to suppress their responses when faced with emotional stimuli, regardless of whether the emotional information is task relevant or irrelevant.

Most previous work on emotional inhibition has examined reactivity to fearful and happy facial emotions. While this provides insight into affective interference caused by differences in valence between these negative and positive emotions, the compared emotions differ in their motivational underpinnings: happiness is an approach-related emotion, but fear is an avoidance-related emotion. In order to distinguish the effect of these motivational differences from those due to the valence of the emotions, a negative social emotion associated with approach tendencies would be a more suitable comparison. Research has shown that anger is related to the approach motivational system (Carver and Harmon-Jones, 2009; Harmon-Jones and Allen, 1998), as it involves a reaction to something aversive, often resulting in an active effort to change this. Thus, a comparison of happiness and anger would help to examine the potential differential effects of positive and negative emotions on adolescent impulse control.

In this study we aimed to extend previous work by investigating how the decreased ability to regulate behaviour in emotional contexts is related to adolescent risk-taking. We examined the effect of emotional information on cognitive control in a group of high risk-taking and a group of low risk-taking adolescents using an emotional go/no-go paradigm (Hare et al., 2008; Somerville et al., 2011). This type of task has been shown to enable reliable assessment of the effects of the affective context on task performance (Schultz et al., 2007). Happy, angry and calm faces were used as stimuli, and participants were instructed to respond to one emotion and ignore the other. We examined the differential effects of happy and angry faces, as well as differences in these effects between the risk-taking groups at both a behavioural and neural level.

Additionally, we used graph-theoretical methods to model functional connectivity between brain regions, to see if these regions play a differential role in emotional impulse control in low and high risk-taking adolescents. Graph-theoretical measures can be used to construct easily computable representations of relatively complex data and are therefore ideally suited to summarize functional connectivity networks (Rubinov and Sporns, 2010). In theory, interpreting task-based functional connectivity networks can be quite complicated as even if just a few regions are used, this involves assessing a vast number of separate potential connections between these regions. Graph theory facilitates this interpretation by allowing examination of characteristics of the network, while also considering the different functional connections between the regions that comprise it. Framing functional connectivity in terms of a network thus diminishes the need to separately look and test for all possible connections between ROIs, and instead computes a small number of neurobiologically meaningful measures (Sporns and Zwi, 2004). Thus, it allows quantification and interpretation of the relative importance a region plays within a network, without having to interpret each of the connections between regions. This makes it a more powerful, and often more intuitive approach. Furthermore, it follows recent calls for a shift from one-to-one mappings of psychological states and regions of the brain towards network-based analyses which recognise the computational roles of the regions involved (Casey, 2015; Pfeifer and Allen, 2016).

In our analyses we used the concept of degree centrality as a measure to describe the relative importance of a region within a functional connectivity network. Degree centrality, which corresponds to the number of connections a given region has, is viewed as the most fundamental network measure, as all other network measures are ultimately linked to it (Bullmore and Sporns, 2009). In a functional connectivity network, connections between regions reflect the magnitude of correlations over time (Rubinov and Sporns, 2010). Consequently, the centrality of a ROI in a functional connectivity network reflects synchronous information processing across the regions it is connected to. Differences between centrality scores thus highlight differences in the importance of a region across task conditions and/or experimental groups. It is important to note that since functional connectivity networks are undirected (i.e. the correlation between region A and B is the same as between B and A), centrality does not reflect the direction of information flow between regions.

In addition to degree centrality, network analyses often examine measures reflecting functional integration in the brain, which reflect the ease with which regions in the network communicate (Rubinov and Sporns, 2010). A frequently used measure is that of the shortest path length between nodes (e.g. brain regions) in a network, with shorter path lengths revealing greater potential for integration between regions. In our analyses we use both centrality and shortest path length measures to examine functional connectivity within an *a priori* defined fronto-striatal network of regions known to be involved in emotion processing and cognitive control.

2. Method

2.1. Participants

The initial sample consisted of 35 healthy adolescents. Data from

one participant was excluded due to incorrect inhibition on all no-go trials in three of the four runs, leaving a sample of 34 participants (20 female, *M* age = 14.57, *SD* age = 0.80, range: 13.21–16.41). Participants were recruited from a larger sample ($N = 323$) in an ongoing longitudinal project examining cognitive and socio-emotional development during adolescence (see e.g.: Baumgartner et al., 2014; Van Batenburg-Eddes et al., 2014). During data collection for this project all participants completed the Columbia Card Task (CCT; Figner et al., 2009). The CCT measures risk-taking under conditions of low and high emotional arousal. During this task, participants draw from a deck of cards, with each card earning or losing them points. The amount of gain and loss and the number of loss cards in the deck varies across trials. Consequently, the CCT is considered a dynamic risk-taking task: the risk parameters change each time a card is turned over. Such tasks are thought to be more reflective of real world behaviour than static tasks, as well as being more engaging for the participant (Weber and Johnson, 2009). In the 'hot' condition of the CCT, participants are shown the outcome of each card after turning it over, and subsequently decide if they wish to continue or move on to the next trial. This condition measures risk-taking under high emotional arousal, as evidenced by increases in physiological measures of arousal such as the skin conductance response (Figner et al., 2009), as well as significant correlations between performance and measures of reward responsiveness (Penolazzi et al., 2012). The CCT has been shown to have good test-retest reliability (Buelow and Barnhart, 2018). All participants in the larger longitudinal sample were ranked based on their deviation from optimal performance during the 'hot' condition of the task (defined as the difference between the mathematically optimal number of cards per condition and the actual number of cards chosen). The top and bottom 30% of the longitudinal sample ($n = 220$), defined as a high risk-taking and low risk-taking group, were subsequently approached to participate in the current study. Of the approached sample 15% were included in the current study, with orthodontic braces forming a constraint for the majority of those who were unable to participate. Participating adolescents did not differ in age from those who were approached but didn't participate ($t(45.59) = 1.04$; $p = .303$), sex ($X^2(1) = 2.87$; $p = .090$), or in CCT scores ($t(44.17) = 0.22$; $p = .823$). In line with our selection criteria, the two risk-taking groups significantly differed on multiple aspects of their CCT performance, both with regards to performance and outcomes. The low risk-taking group chose a close to optimal number of cards ($M = 0.14$, $SD = 1.00$) while the high risk group selected more cards than optimal ($M = 7.47$, $SD = 1.01$; difference low vs high: $t(31.44) = 21.27$, $p < .001$). The low risk group ended trials before a loss card was drawn (or turned over no cards during the trial) on an average of 71.2% ($SD = 10.0\%$) of trials, while the high risk group did so on only 48.2% ($SD = 10.3\%$) of trials. This difference was significant $t(31.28) = 6.581$; $p < .001$. In addition, the low risk group finished the task with average earnings of −0.12 euro (SD = 7.37) while the high risk group earned an average of -7.53 euro (SD = 7.67). This difference was also significant $t(31.16) = 2.860$; $p = .007$.

All participants were typically developing, had normal vision, reported no neurological or psychiatric disorders and had no contra-indications for MRI. Demographic characteristics are reported in Table 1. Age and sex did not differ between the two risk-taking groups (age: $t(30.98) = 1.17$, $p = .249$; sex: $X^2(1) = 0.08$, $p = .773$). Consent for all phases of the project was obtained from the Ethical Committee of the University of Amsterdam Faculty of Behavioural and Social Sciences. All participants and their guardians provided written informed consent prior to participation.

Table 1
Participant characteristics.

	Low risk-taskers	High risk-takers
N	18 (11 females)	16 (9 females)
Age (*M* (SD))	14.72 (.77)	14.40 (0.82)
CCT score[a]	0.14 (1.00)	7.47 (1.01)

[a] CCT score was calculated as the deviation from optimal performance across conditions.

2.2. Measures

2.2.1. Task development

The emotional go/no-go task (Hare and Casey, 2005; Somerville et al., 2011) comprising calm, happy and angry facial expressions was refined during an initial pilot phase to ensure comparable levels of emotional valence between conditions in adolescents. A group of 126 adolescents were recruited from local schools specifically for the pilot. Participants rated the valence of 96 (32 per emotion) calm, happy and angry faces from the NimStim set of facial expressions (Tottenham et al., 2009) using a Likert scale ranging from −4 (strongly negative) to +4 (strongly positive). Participants reported how realistic they found the expressions using a 7-point Likert scale (1 = completely unrealistic, 7 = very realistic).

In the happy and angry conditions, the data were used to select the 10 faces (5 male, 5 female) which the participants found most realistic and with the highest absolute valence ratings in the intended direction. Mean valence ratings were balanced between the happy and angry conditions to ensure that differences between the emotions were not due to the intensity of the emotions displayed. A set of 10 faces (5 male, 5 female) was also selected for the calm condition, based on those faces rated by the participants as most realistic, and with the most neutral valence ratings. Calm faces were used as neutral stimuli, as previous research has shown that neutral faces are often characterised by participants as portraying negative emotions (Herba and Phillips, 2004). All conditions comprised a combination of open and closed mouths.[2]

2.2.2. Experimental task

A modified emotional go/no-go task was created with stimuli selected based on data from the pilot phase (Fig. 1). Within a go/no-go paradigm participants are instructed to press a button as quickly as possible when shown a 'go' (i.e., target) stimulus and to inhibit their response by not pressing the button when shown a 'no-go' (i.e., non-target) stimulus.

The rapid event-related task comprised four blocks presented across four different runs. Each block contained two facial emotions (calm and happy, or calm and angry), one instructed to be the target and one as the non-target stimulus, leading to four conditions: (i) happy go/calm no-go, (ii) happy no-go/calm go, (iii) angry go/calm no-go, and (iv) angry no-go/calm go.

At the start of each block participants were shown a screen indicating the target emotion for that block, and reminding them not to respond to other emotions. Each block consisted of 16 trials, with targets ('go') occurring on 75% of these trials, resulting in a total of 96 angry/happy go trials (48 happy, 48 angry), 32 angry/happy no-go trials (16 happy, 16 angry), 96 calm go trials and 32 calm no-go trials across the four runs (256 trials in total). Trials within a block, and block order within a run, were randomized across participants. Each trial started with a face, which was displayed for 500 ms, followed by a fixation cross which was displayed for a variable interstimulus interval between 1500 ms–2500 ms (in steps of 500 ms). After the last trial of a block, the fixation cross was displayed for 10 s. During the last trial of a run the fixation cross was displayed for 20 s in order to acquire the final BOLD response in full.

The task was presented in Presentation using a projection screen and mirror within the head coil. Responses were recorded using a response box attached to the participant's respiratory belt. Participants

[2] A full list of the selected stimuli is available from the first author upon request.

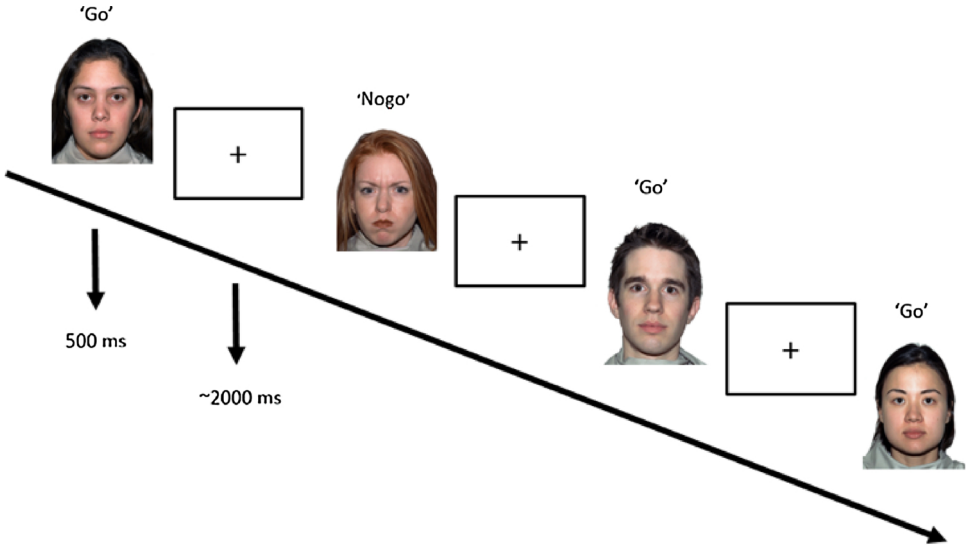

Fig. 1. Go/no-go task design. The figure displays three trials in a run with calm faces as target stimuli and angry faces as non-targets.

responded with their right index finger.

2.3. Image acquisition

Participants were scanned with a 3 T Philips Achieva XT with a 32-channel receiver head coil. Functional images were acquired using a single shot GE-EPI sequence (MS-FFE single shot EPI, TE = 27.63, FA = 76.1, SENSE (AP) = 2, FOV = 240^2, Bandwidth = 36.2 Hz) with a voxel size of 3*3*3 mm (37 slices with an interslice gap of 0.3 mm) and a TR of 2 s. Structural images were acquired using a fast MPRage sequence (3DFFE multishot TFE, TR = 8.2, TE = 3.8, FA = 8, Sense P (RL) = 2.5, Sense S(FH) = 2, FOV = 240*188, Bandwidth = 191.4 Hz), with a voxel size of 1*1*1 mm (220 slices).

2.4. Analyses

2.4.1. Behavioural data analysis

Four behavioural outcome measures were computed based on the go/no-go task: proportion of hits (correct response to go stimulus), misses (failure to respond to go stimulus), correct rejections (correct withholding of response to no-go stimulus) and false alarms (incorrect response to no-go stimulus) across all trials. Mean reaction times for hits and false alarms were also calculated. Differences in performance between the risk-taking groups on trials classified as misses, false alarms, and reaction times on hit and false alarm trials, were analysed using a 3 (Emotion: calm, happy, angry) × 2 (Risk-taking: high, low) ANOVA (linear mixed model with a random intercept across participants). Post-hoc paired samples *t*-tests were used to further examine significant interactions.

2.4.2. Imaging data analysis

Pre-processing and General Linear Model (GLM) analyses were performed using FSL (Jenkinson et al., 2012). Functional images were brain extracted (Smith, 2002), motion corrected and registered to the structural images using linear registration (FLIRT (BBR 12 dof), Jenkinson and Smith, 2001). For the group analyses images were registered to standard MNI space. Time-series were pre-whitened and low-pass filtered (90 s). Spatial smoothing was applied using a 6 mm FWHM kernel. Blood Oxygenation Level Dependent (BOLD) responses were modeled as a double-gamma Haemodynamic Response Functions (HRF) with a temporal derivative to account for differences in slice acquisition time. The GLM design matrix included six main regressors (angry go, angry no-go, happy go, happy no-go, calm go, and calm no-go) and two regressors of no interest (errors and instruction screens). Motion regressors (6) derived from MCFLIRT (Jenkinson et al., 2002) were added to the GLM design matrix as regressors of no interest, and volumes with excessive motion (Root mean square (RMS) > 0.75 percentile + 1.5*Interquartile Range (IQR) using *fsl_motion_outliers*) were regressed out using additional confound regressors. Mean number of volumes censored per run was 6.07 (*SD* = 3.40, Range = (223)). Average motion over all runs and subjects was 0.73 mm (*SD* = 0.88). In five runs, maximum motion exceeded 3 mm (two runs maximum motion was 5.26 mm, in one run motion was 4.39, in one run motion was 3.62, and in one run motion was 3.28 mm). Motion in these volumes was also censored. Four out of 136 runs (4 runs × 34 subjects) were discarded due to no correct inhibitions on happy no-go trials (3 runs) or no correct inhibitions on angry no-go trials (1 run).

A-priori region-of-interest (ROI) masks were generated bilaterally for the amygdala, inferior frontal gyrus (IFG) (FSL Harvard Oxford Atlas, 50% probability threshold), dorsal striatum and ventral striatum (FSL Striatum Atlas). These regions have been reported previously as being activated during emotional go/no-go tasks and implicated in cognitive control (Hare et al., 2008; Somerville et al., 2011).

To confirm that regions previously implicated in emotional go/no-go paradigms were also activated in our sample, two whole-brain GLM analyses (Familywise Error (FWE) corrected with a cluster-forming threshold of $Z > 3.1$; cluster-wise $p < .05$; Worsley, 2001) were examined. First, an emotional (angry + happy) > calm contrast was used to examine involvement of regions usually active in emotional paradigms. Second, a no-go > go contrast was used to examine the contribution of regions associated with inhibitory control.

To examine differences between the risk-taking groups, masks were constructed as a 4 mm radius sphere centred at the peak voxel in each a-priori defined ROI for each of the six trial types and subjects separately. Parameter estimates were extracted from this sphere for each ROI for each of the six trial types (calm go, calm no-go, happy go, happy no-go, angry go, angry no-go). An overview of the MNI coordinates of the spheres extracted from each ROI is given in Table 2. The extracted values were used in a 3 (Emotion: calm, happy, angry) × 2 (Trial Type: go, no-go) × 2 (Risk-taking: high, low) ANOVA (linear mixed model with a random intercept across participants). Where appropriate *t*-tests were used to further examine significant interactions.

The ROI analyses were followed by an analysis to estimate functional connectivity in each condition between the eight regions of interest for each individual participant. We used a graph-theoretical approach using beta-series to determine connectivity between ROIs. This

Table 2
Median (bold), minimum and maximum values of the peak-voxel coordinates (across subjects, split for each condition) within each predefined Region-of-Interest. All coordinates are in MNI space.

Region-Of-Interest		Calm Go			Calm No-go			Happy Go			Happy No-go			Angry Go			Angry No-go		
		x	y	z	x	y	z	x	y	z	x	y	z	x	y	z	x	y	z
Amygdala Left	median	**−22**	**−2**	**−14**	**−22**	**−2**	**−14**	**−22**	**−2**	**−14**	**−24**	**0**	**−16**	**−22**	**−2**	**−14**	**−22**	**−2**	**−14**
	min	−16	−10	−24	−16	−10	−24	−16	−10	−24	−16	−10	−24	−16	−10	−24	−16	−10	−24
	max	−34	2	−12	−34	2	−10	−34	2	−10	−34	2	−10	−34	2	−10	−34	2	−10
Amygdala Right	median	**16**	**−2**	**−14**	**18**	**0**	**−14**	**18**	**−2**	**−12**	**18**	**0**	**−14**	**18**	**−2**	**−14**	**18**	**−2**	**−14**
	min	24	−10	−24	24	−10	−24	28	−10	−24	28	−10	−24	24	−10	−24	28	−10	−22
	max	12	4	−8	12	4	−10	12	4	−10	12	4	−10	12	4	−10	12	4	−8
Dorsal Striatum Left	median	**−14**	**2**	**12**	**−20**	**8**	**4**	**−16**	**6**	**8**	**−16**	**6**	**6**	**−18**	**4**	**12**	**−18**	**6**	**8**
	min	−8	−16	−10	−8	−16	−10	−8	−16	−10	−8	−18	−10	−10	−18	−10	−8	−18	−10
	max	−34	16	26	−34	20	24	−34	14	24	−34	16	24	−34	24	26	−32	26	22
Dorsal Striatum Right	median	**10**	**6**	**10**	**10**	**10**	**10**	**12**	**2**	**10**	**10**	**4**	**12**	**12**	**4**	**12**	**12**	**4**	**10**
	min	30	−18	−8	30	−18	−8	30	−10	−6	28	−10	−8	30	−16	−8	30	−10	−6
	max	6	26	28	4	20	28	6	16	28	6	26	28	4	24	26	6	24	24
Ventral Striatum Left	median	**−14**	**10**	**−10**	**−14**	**10**	**−8**	**−14**	**12**	**−8**	**−14**	**10**	**−6**	**−16**	**10**	**−10**	**−14**	**10**	**−6**
	min	−6	8	−12	−6	8	−12	−6	8	−12	−6	8	−12	−6	8	−12	−6	8	−12
	max	−22	22	2	−22	22	2	−20	22	2	−22	18	2	−22	22	2	−20	22	2
Ventral Striatum Right	median	**10**	**10**	**−8**	**12**	**12**	**−8**	**14**	**12**	**−8**	**12**	**10**	**−8**	**10**	**12**	**−6**	**12**	**12**	**−6**
	min	18	8	−10	18	8	−10	18	8	−10	18	8	−10	18	8	−10	18	8	−10
	max	2	22	2	4	22	2	4	22	2	4	22	2	4	22	2	2	22	2
Inferior Frontal Gyrus Left	median	**−56**	**18**	**14**	**−56**	**18**	**12**	**−56**	**20**	**10**	**−56**	**20**	**8**	**−56**	**18**	**10**	**−56**	**20**	**14**
	min	−52	12	0	−50	12	2	−52	12	0	−52	12	0	−52	12	0	−52	12	0
	max	−58	36	28	−60	36	28	−58	36	28	−60	36	28	−60	30	28	−60	36	28
Inferior Frontal Gyrus Right	median	**54**	**22**	**14**	**52**	**20**	**8**	**54**	**22**	**10**	**52**	**20**	**12**	**54**	**22**	**14**	**52**	**20**	**8**
	min	58	14	0	58	14	0	58	14	0	58	14	0	58	14	0	58	14	0
	max	48	34	28	48	34	30	52	32	30	48	34	30	48	34	28	48	34	30

approach entails constructing a network with the 8 ROIs for each condition and each subject, with the nodes of the network defined by the 8 ROIs and the connections between the nodes defined by the correlation of the beta-series of these ROIs. To construct the network, we first summarized activity over time by taking the first eigenvector of all the time-series of each voxel within each ROI (Friston et al., 2006). This resulted in a time-series characteristic of each of the eight ROIs. On these time-series single trial estimates of activity were calculated using the Least-Squares Single (LSS) method by Mumford et al. (2012) and Turner et al. (2012). This method entails performing a GLM for each trial in the experiment separately. In each GLM the trial of interest (e.g., the first calm no-go trial in a run) is modelled as a single regressor, with the other trials of the same stimulus type (e.g., the second through to the last calm no-go trial) as a second regressor. Other trials of other stimulus types (i.e. conditions) are added as additional regressors, as are the confound regressors (e.g. motion parameters) used in the ROI analyses. This resulted in an estimate of the amplitude of activation for each single trial in the experiment. Single-trial estimates where then concatenated over runs within each condition, resulting in an 'amplitude' time-series for each condition for each subject in the experiment.

Next, for each condition in the experiment, we defined a network with the eight ROIs as nodes and the correlation between the amplitude time-series of the different ROIs as edges. The resulting network thus indicates the functional connectivity between brain regions within a certain condition. To overcome possible artefacts of differing lengths of the amplitude time-series – for example, the task consisted of more calm-go trials than angry no-go trials – we used a bootstrap approach. Each amplitude time-series was restricted to have a maximum length of 16 (the theoretical maximum number of correct trials of the condition with the lowest number of trials, 4 trials × 4 runs). At every bootstrap iteration we sampled 16 data points from the amplitude time-series of conditions with more than 16 trials. With these resampled amplitude time-series we constructed the network. We repeated the resampling and network construction 1000 times and averaged the functional connectivity estimates (i.e. the correlations between ROIs within a condition) over these 1000 iterations. This resulted in an 'average' network for each condition for each subject.

To assess the resulting functional connectivity networks for each condition we looked at a measure of the relative importance of the ROIs (i.e. *nodes*) within a network, termed *centrality* (Rubinov and Sporns, 2010). A node's centrality can be interpreted as the relative importance of the node within the network. Mathematically, it is the weighted sum of all the correlations between that node and the other nodes. In terms of a functional connectivity network (with the ROIs being nodes and the correlations between ROIs the weighted edges), a high level of centrality means that this ROI has a higher number and/or stronger correlations with the other nodes in the network. High centrality thus means that this region is more strongly functionally connected and/or has more functional connections with the other nodes. We calculated degree centrality and shortest path length for each ROI within each average network, resulting in an estimate of the importance of a region for each condition and each subject. These estimates were entered as dependent variables in a linear mixed model with Risk group as between-subjects factor, Emotion and Trial-Type as within-subjects factors and a random intercept over subjects. Analyses were performed separately for each ROI, similar to the ROI analyses in the previous section.

To further specify if differences in centrality are due to an overall increase of connections or due to large differences in the connectivity strength of specific connections, we performed the same analysis on binarized correlation matrices using different correlation thresholds ($r > 0.1$, 0.3, 0.5, 0.7, or 0.9). This method is useful to filter out the influence of small/weak links within the network. As thresholds are determined somewhat arbitrarily, we follow the convention that multiple thresholds are used (see Rubinov and Sporns, 2010). In the binarized network all correlations below the threshold (i.e. subthreshold) were set to zero, all the supra-threshold correlations were set to 1. The number of incoming supra-threshold connections was taken as the dependent variable.

To visualize the connectivity patterns, we plotted the graphs for each of the six conditions for both risk groups. Network analyses were performed using the R-package *qgraph* (Epskamp et al., 2012), centrality measures were calculated using the method by Opsahl et al. (2010) as implemented in *qgraph*.

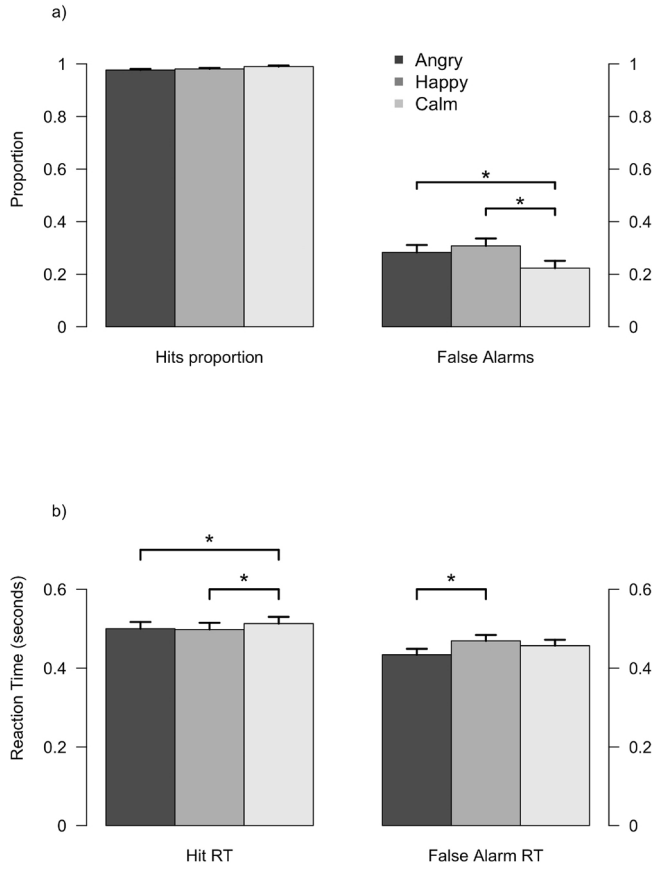

Fig. 2. Hit and false alarm responses per emotion (a) proportion of hits and false alarms, (b) reaction times for hit and false alarm trials.

To correct for inflated type I error rates across our ROI analyses for each of the 8 regions we used Bonferroni correction on the number of ROIs ($\alpha = 0.05/8 = 0.0063$; trends $\alpha = 0.0125$). For consistency, p-values in the text are uncorrected values. To show the specificity of our ROI and connectivity analyses we performed these analyses again using control regions where task effects weren't expected. Results of these analyses are shown in Appendix A.

3. Results

3.1. Behavioural results

The analyses showed a difference between the target emotional expression in participants' false alarm rates (main effect of Emotion: $F(2, 64) = 6.058$, $p = .004$). Post hoc paired samples t-tests showed more false alarms in response to angry non-targets relative to calm non-targets ($t(33) = -2.476$, $p = .019$), and more false alarms to happy non-targets in comparison to calm non-targets ($t(33) = -3.610$, $p = .001$; Fig. 2a). The number of miss trials differed marginally between emotions ($p = .065$). Post-hoc tests showed that more misses occurred in angry trials than in calm trials ($t(33) = 2.226$, $p = .033$). No difference was found between the groups ($p = .600$) in the number of miss trials. Subsequent analyses of reaction times showed a similar main effect of Emotion on hit trials ($F(2, 64) = 4.863$, $p = .011$), due to faster responses to angry ($t(33) = 2.392$, $p = .023$) and happy ($t(33) = 3.128$, $p = .004$) compared to calm trials. Reaction times for false alarms differed between emotions ($F(2, 54) = 3.334$, $p = .043$), due to faster responses to happy faces than angry faces ($t(29) = -2.071$, $p = .047$; Fig. 2b). No differences were found when comparing the emotional to calm stimuli, suggesting that the heightened false alarm rate in the emotional conditions was not due to a speed accuracy trade-off. No differences were found between risk-taking groups for any of the behavioural or reaction time indices.

3.2. Imaging results

3.2.1. Whole brain analysis

Initial whole brain analyses (FWE cluster corrected, $Z > 3.1$, $p < .05$) confirmed that regions previously implicated in go/no-go and emotional task performance were also activated in our sample. For the no-go > go contrast, clusters of activation were found in the temporal cortex, dorso- and ventrolateral prefrontal cortex, parietal cortex and the dorso-anterior cingulate cortex (Fig. 3, coordinates in Table 3). For the emotional (happy + angry) > calm contrast, one cluster of activation was found in the temporal occipital fusiform cortex (Fig. 4, coordinates in Table 4). Fig. 5 shows an overview of the a-priori ROIs (blue) and the actual activation values in our sample (red, FWE cluster-wise $p < .05$). For the emotional > calm contrast no overlap was found. For the no-go > go contrast overlap between a-priori ROIs concentrated on the amygdala.

3.2.2. Region-of-interest analysis

Further examination targeting the a priori ROIs revealed differences in the magnitude of activation between go and no-go trials in the right IFG ($F(1, 160) = 9.593$, $p = .002$), and in the right amygdala at trend level ($F(1, 160) = 6.383$, $p = .012$). In these regions activation was greater during no-go trials, which required higher levels of cognitive control, than during go trials.

Analyses also showed a bilateral interaction effect of Trial Type and Emotion in the left ventral striatum ($F(2, 160) = 3.367$, $p = .037$) and right ventral striatum ($F(2, 160) = 3.536$, $p = .031$). While it did not meet the Bonferroni adjusted p-value, it did fall within uncorrected thresholds. We tentatively report the results here as Bonferroni corrections are known to be conservative when tests are correlated (Poldrack et al., 2011, p. 117), similar effects were found bilaterally, and the findings are in line with previous research demonstrating that the ventral striatum is known to play an important role in reward processing (e.g. Delgado, 2007). Post hoc t-tests showed this was due to greater activation during happy no-go than happy go trials in right/left

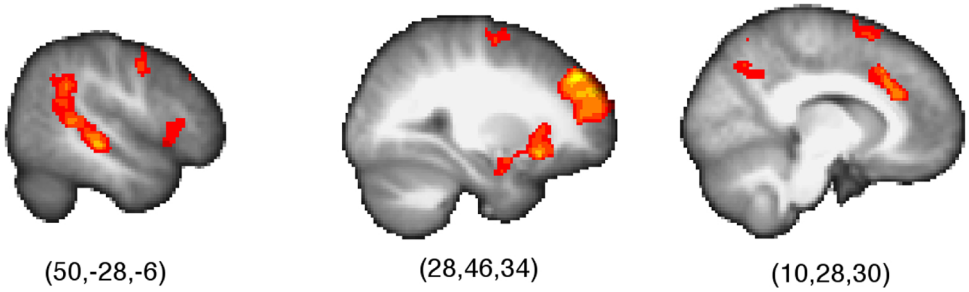

Fig. 3. Whole brain activation for the no-go > go contrast (FWE cluster corrected, Z > 3.1, $p < .05$) showing activation in the right temporal cortex, the right dorso- and ventrolateral prefrontal cortex, right parietal cortex and the right dorso-anterior cingulate cortex. Coordinates are in MNI space.

Table 3
MNI Coordinates and z-values for significantly activated clusters (FWE corrected $p < .05$, cluster forming threshold Z > 3.1) for the no-go > go contrast.

no-go > go contrast Region	z-value	x	y	z
Middle Temporal Gyrus/Angular Gyrus/	5.25	50	−26	−6
Supramarginal Gyrus (Right)	5.19	68	−40	24
(2408 voxels)	4.79	60	−46	30
	4.73	50	−44	8
	4.63	62	−32	36
	4.62	66	−50	18
Frontal Pole (Right)	5.85	30	46	38
(1975 voxels)	5.61	30	56	28
	5.10	38	50	16
	5.09	34	48	14
	4.58	26	54	16
	4.46	28	58	18
Frontal Orbital Cortex / Insula (Right)	6.01	32	20	−10
(1510 voxels)	5.82	34	26	4
	5.15	42	16	−4
	4.11	20	−4	−12
	4.05	30	2	−14
	3.97	24	−2	−14
Superior Frontal Gyrus (Right)	4.66	20	0	68
(798 voxels)	4.50	14	10	62
	4.45	18	−10	62
	4.03	8	20	66
	3.76	30	−6	60
	3.22	36	−4	68
Frontal Orbital Cortex (Left)	5.00	−32	28	0
(498 voxels)	4.79	−28	20	−12
	3.56	−20	10	−18
Precuneus Cortex (Right)	3.74	10	−66	44
(374 voxels)	3.62	8	−64	36

ventral striatum (right ventral striatum: $t(33) = -2.650$, $p = .012$; left ventral striatum: $t(33) = -2.180$, $p = .037$). No trial type differences were found for the calm or angry conditions in these areas. With regards to risk-taking groups the main effects of Emotion and Trial Type, as well as the interactions between these effects did not differ between the groups. Estimated marginal means and standard errors are displayed in Table 5.

3.2.3. Connectivity analysis

Analyses of functional connectivity revealed a three-way Emotion by Trial Type by Risk Group interaction in the dorsal striatum (Left dorsal striatum: $F(2,160) = 5.198$; $p = .006$; Right dorsal striatum: $F(2,160) = 5.233$; $p = .006$). Further inspection of these effects within the risk-taking groups shows that the Emotion by Trial Type interaction is reversed for the high risk-taking group as compared to the low risk-taking group (see Table 6 and Figs. 6 and 7). For participants in the low risk-taking group the dorsal striatum has lower centrality in the calm go trials compared to the calm no-go trials, while centrality scores where lower for emotional no-go trials than go trials. This effect is reversed for participants in the high risk-taking group: they showed lower centrality in the calm no-go trials than go trials, and the centrality of the dorsal striatum increased as the emotional demands of the task increased (i.e. from emotional go to no-go trials). This effect appeared stronger for angry than happy trials. The same three-way interaction effect was observed for the shortest path length (left dorsal striatum: $F(2,160) = 5.575$; $p = .005$; right dorsal striatum: $F(2,160) = 5.552$; $p = .005$), corroborating our degree centrality findings, where higher centrality is associated with shorter path lengths. Marginal means are displayed in Table 7.

Table 4
MNI Coordinates and z-values for significantly activated clusters (FWE corrected $p < .05$, cluster forming threshold Z > 3.1) for the emotional > calm contrast.

emotional > calm contrast Region	z-value	x	y	z
Temporal Occipital Fusiform Gyrus (Right)	5.00	44	−42	−14
(383 voxels)	3.99	40	−50	−16
	3.64	44	−60	−10
	3.47	34	−46	−18
	3.25	38	−60	−10
	3.25	48	−58	−18

To pinpoint if the differences in centrality scores in the left and right dorsal striatum are due to a few stronger connections or due to a smaller increase in many connections, we performed additional analyses on binarized networks using different thresholds. For the binarized networks we see the same three-way interaction with correlation thresholds between 0.2 and 0.45 for the right dorsal striatum, and for thresholds between 0.3 and 0.5 for the left dorsal striatum. This indicates that the number of incoming connections with a correlation strength between these numbers are driving the centrality differences. Appendix B shows the average connection strength of the connections between the left and right dorsal striatum with the other ROIs for the Emotion, Trial Type and Risk-taking groups. There is no indication that one specific connection is driving the centrality differences, but that it is more of an overall increase in connectivity strength of multiple ROIs. As can be seen for example in the left dorsal striatum, the higher centrality differences between the risk-taking groups in the angry no-go condition are driven by the amygdala (strength from approximately 0.20 to 0.45) and by the increased connection between the dorsal striatum and right IFG and ventral striatal areas (from approximately 0.40 to 0.52). A supplementary analysis where we subsequently left out one of the ROIs connecting to the dorsal striatum and repeated the centrality analysis, showed that the ventral striatal areas were most important in driving the centrality differences. The IFG (bilateral) and left amygdala were most important after that, while the right amygdala

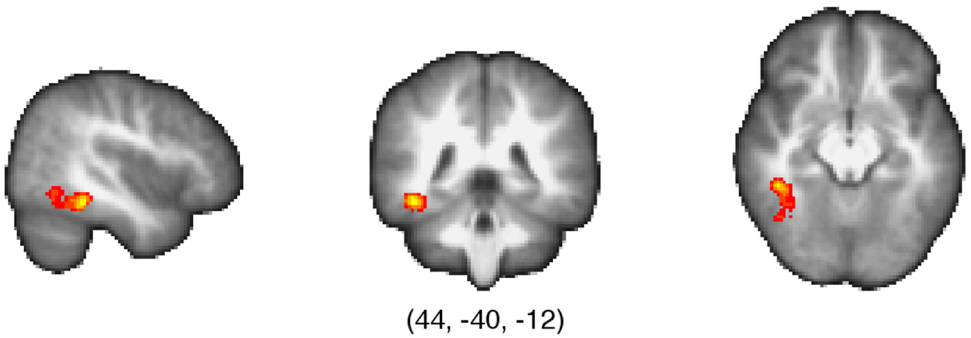

Fig. 4. Whole brain activation for the emotional (angry + happy) > calm contrast (FWE cluster corrected, Z > 3.1, $p < .05$) showing activation in the temporal occipital fusiform cortex. Coordinates are in MNI space.

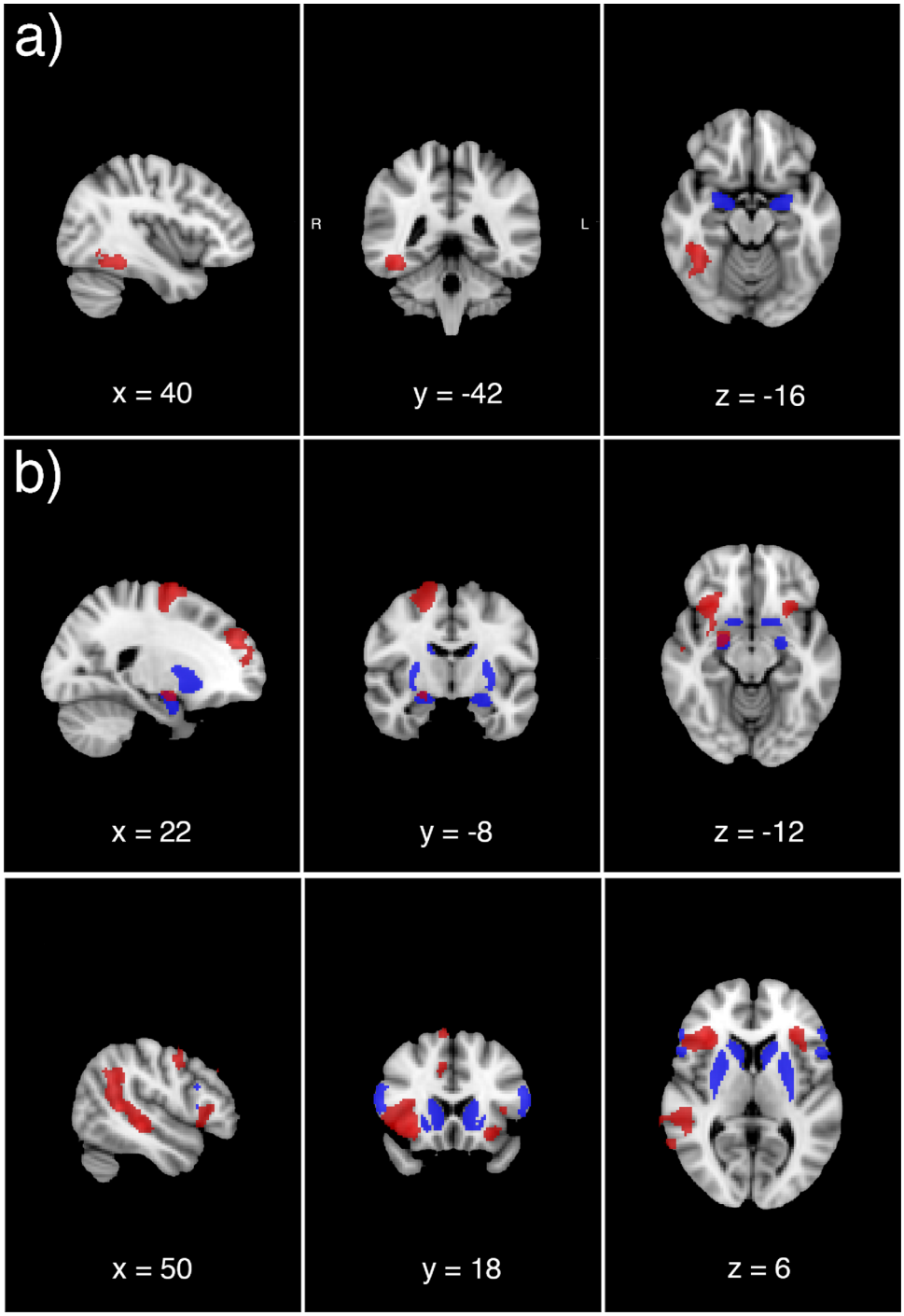

Fig. 5. Overlap between a-priori defined ROIs (blue) and the two whole brain contrasts (red). Top panel (a) indicates overlap for the emotional > calm contrast. Lower panels (b) indicate overlap with the no-go > go contrast, showing some overlap with the right amygdala. All coordinates are in MNI space (For interpretation of the references to colour in this figure legend, the reader is referred to the web version of this article).

was least important.

4. Discussion

In the present study we used an emotional go/no-go paradigm to investigate the effect of salient appetitive and aversive emotional information on cognitive control in a group of high risk-taking and a group of low risk-taking adolescents. Consistent with prior work using a similar paradigm (e.g. Dreyfuss et al., 2014; Somerville et al., 2011), we show that emotional cues decreased levels of cognitive control. While analysis of activation in our *a priori* regions of interest did not conclusively demonstrate differences between the risk-taking groups, analyses of functional connectivity did reveal differences, specifically in the interactions between the dorsal striatum and other regions. Our findings suggest that variance in fronto-striatal circuitry may underlie the observed individual differences in risk-taking behaviour.

4.1. The influence of emotional cues on cognitive control

The behavioural data showed that when the emotional demands of the task were high, participants made more inhibitory errors. These behavioural effects did not differ between the risk-taking groups. The

Table 5
Estimated Marginal Means of the activation of each region-of-interest (amygdala, inferior frontal gyrus (IFG), dorsal- and ventral striatum). Standard Errors are in brackets.

Trial Type	Emotion	Risk Group	Amygdala (left)		Amygdala (right)		IFG (left)		IFG (right)		Dorsal Striatum (left)		Dorsal Striatum (right)		Ventral Striatum (left)		Ventral Striatum (right)	
			Mean	SE	Mean	SE	Mean	SE	Mean	SE	Mean	SE	Mean	SE	Mean	SE	Mean	SE
Go	Angry	High risk	160.23	(57.21)	177.54	(54.85)	−160.76	(67.50)	−12.61	(61.85)	−28.73	(62.52)	−108.02	(57.48)	−62.13	(46.08)	−103.13	(43.95)
		Low risk	222.28	(53.94)	155.11	(51.71)	−20.60	(63.64)	−51.32	(58.31)	−45.09	(58.94)	−55.65	(54.19)	−21.07	(43.44)	−54.36	(41.43)
	Calm	High risk	84.91	(57.21)	103.70	(54.85)	−95.11	(67.50)	−99.69	(61.85)	7.24	(62.52)	−69.12	(57.48)	−31.31	(46.08)	−44.63	(43.95)
		Low risk	117.94	(53.94)	128.18	(51.71)	53.20	(63.64)	−15.65	(58.31)	7.27	(58.94)	−52.28	(54.19)	−35.58	(43.44)	−17.74	(41.43)
	Happy	High risk	135.71	(57.21)	23.14	(54.85)	−89.92	(67.50)	−75.40	(61.85)	−33.64	(62.52)	−67.41	(57.48)	−73.30	(46.08)	−91.56	(43.95)
		Low risk	86.34	(53.94)	37.90	(51.71)	−33.06	(63.64)	−151.23	(58.31)	−64.32	(58.94)	−67.41	(54.19)	−58.61	(43.44)	−100.46	(41.43)
No-go	Angry	High risk	134.37	(57.21)	210.89	(54.85)	−81.15	(67.50)	119.51	(61.85)	−103.66	(62.52)	−69.17	(57.48)	−63.29	(46.08)	−39.99	(43.95)
		Low risk	135.11	(53.94)	252.66	(51.71)	41.46	(63.64)	70.66	(58.31)	−34.49	(58.94)	−88.62	(54.19)	−43.01	(43.44)	−4.40	(41.43)
	Calm	High risk	95.24	(57.21)	115.25	(54.85)	−58.88	(67.50)	−39.24	(61.85)	−5.12	(62.52)	−52.80	(57.48)	−75.64	(46.08)	−75.51	(43.95)
		Low risk	81.72	(53.94)	84.63	(51.71)	−68.11	(63.64)	−55.08	(58.31)	−111.16	(58.94)	−54.98	(54.19)	−82.33	(43.44)	−56.45	(41.43)
	Happy	High risk	208.13	(57.21)	278.98	(54.85)	77.57	(67.50)	86.89	(61.85)	132.96	(62.52)	94.83	(57.48)	74.79	(46.08)	62.65	(43.95)
		Low risk	88.89	(53.94)	113.20	(51.71)	−11.01	(63.64)	−55.95	(58.31)	−81.42	(58.94)	−99.24	(54.19)	−10.66	(43.44)	−30.49	(41.43)

Table 6
Estimated Marginal Means of the centrality values of each region-of-interest (amygdala, inferior frontal gyrus (IFG), dorsal- and ventral striatum). Standard Errors are in brackets.

Trial Type	Emotion	Risk Group	Amygdala (left)		Amygdala (right)		IFG (left)		IFG (right)		Dorstal Striatum (left)		Dorsal Striatum (right)		Ventral Striatum (left)		Ventral Striatum (right)	
			Mean	SE	Mean	SE	Mean	SE	Mean	SE	Mean	SE	Mean	SE	Mean	SE	Mean	SE
Go	Angry	High risk	2.860	(0.22)	3.245	(0.22)	3.117	(0.24)	3.160	(0.24)	3.415	(0.24)	3.493	(0.23)	3.211	(0.22)	3.150	(0.22)
		Low risk	2.709	(0.20)	2.802	(0.21)	2.697	(0.23)	2.566	(0.23)	3.548	(0.22)	3.474	(0.22)	2.947	(0.21)	3.077	(0.21)
	Calm	High risk	2.960	(0.22)	3.111	(0.22)	3.097	(0.24)	3.114	(0.24)	3.713	(0.24)	3.692	(0.23)	3.288	(0.22)	3.202	(0.22)
		Low risk	2.605	(0.20)	2.738	(0.21)	2.207	(0.23)	2.346	(0.23)	3.154	(0.22)	3.142	(0.22)	2.864	(0.21)	2.820	(0.21)
	Happy	High risk	2.742	(0.22)	2.939	(0.22)	2.893	(0.24)	2.770	(0.24)	3.487	(0.24)	3.551	(0.23)	3.116	(0.22)	3.078	(0.22)
		Low risk	2.838	(0.20)	2.923	(0.21)	2.435	(0.23)	2.446	(0.23)	3.385	(0.22)	3.413	(0.22)	3.146	(0.21)	3.124	(0.21)
No-go	Angry	High risk	3.261	(0.22)	3.430	(0.22)	2.994	(0.24)	3.224	(0.24)	3.954	(0.24)	3.933	(0.23)	3.647	(0.22)	3.617	(0.22)
		Low risk	2.850	(0.20)	2.829	(0.21)	2.759	(0.23)	2.584	(0.23)	3.248	(0.22)	3.137	(0.22)	3.034	(0.21)	3.124	(0.21)
	Calm	High risk	2.689	(0.22)	3.024	(0.22)	2.910	(0.24)	2.860	(0.24)	3.322	(0.24)	3.319	(0.23)	3.015	(0.22)	2.996	(0.22)
		Low risk	2.876	(0.20)	2.909	(0.21)	2.739	(0.23)	2.626	(0.23)	3.450	(0.22)	3.462	(0.22)	3.245	(0.21)	3.195	(0.21)
	Happy	High risk	2.635	(0.22)	2.994	(0.22)	2.932	(0.24)	3.218	(0.24)	3.450	(0.24)	3.644	(0.23)	3.626	(0.22)	3.173	(0.22)
		Low risk	2.669	(0.20)	2.906	(0.21)	2.475	(0.23)	2.488	(0.23)	3.044	(0.22)	3.180	(0.22)	3.203	(0.21)	3.094	(0.21)

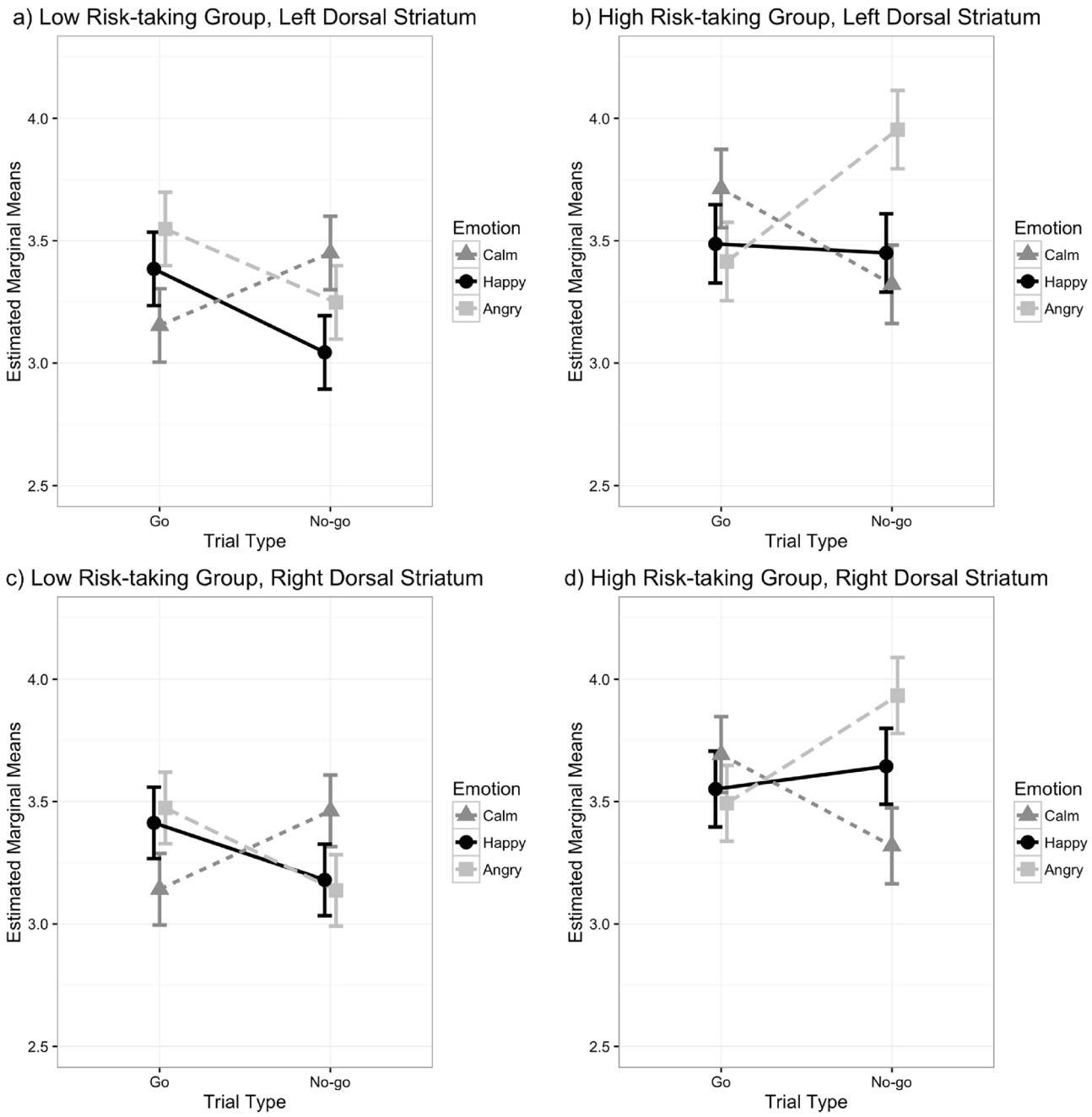

Fig. 6. Mean centrality scores of the dorsal striatum (left and right) split by Trial Type (go, no-go) and Emotion (calm, happy, angry) for both risk-taking groups. Error-bars indicate one standard error (Cousineau within-subjects, (Cousineau, 2005)) above/below the mean.

results suggest that both positive and negative emotional information disrupt adolescents' ability to inhibit a prepotent behavioural response. This is however not the case for neutral emotional information. Previous work in adolescents has shown that appetitive stimuli, (i.e., happy faces) facilitate approach responses and decrease reaction times (Somerville et al., 2011). Consequently, adolescents are often unable to override this strong approach motivation, leading to behavioural errors in the case of a go/no-go paradigm such as the one used in our study. A growing body of evidence suggests that adolescents also show decreased performance when confronted with negatively-valenced stimuli (Cohen-Gilbert and Thomas, 2013; Dreyfuss et al., 2014; Galvan and McGlennen, 2013; Urben et al., 2012). While much of this previous work has focused on fearful or threatening faces, our results show that this is also the case for negatively valenced approach emotions, such as anger, evidenced by the increased errors and faster responses in response to angry compared to calm faces. This finding suggests that both positively and negatively valenced approach stimuli disrupt inhibitory control. However, there may be situations in which the effects of heightened emotional arousal during adolescence can be beneficial. Recent work suggests that adolescents' increased sensitivity to rewards enables them to achieve adult levels of simple forms of cognitive control when offered an incentive to do so (Padmanabhan et al., 2011), but not for more complex forms (Insel et al., under review). In our sample the observed behavioural effects under emotional conditions did not differ between the low and high risk-taking groups. This failure to find a behavioural effect could be due to all participants in our relatively small sample generally performing well on the task and making few errors, thus leaving little room for individual differences in performance.

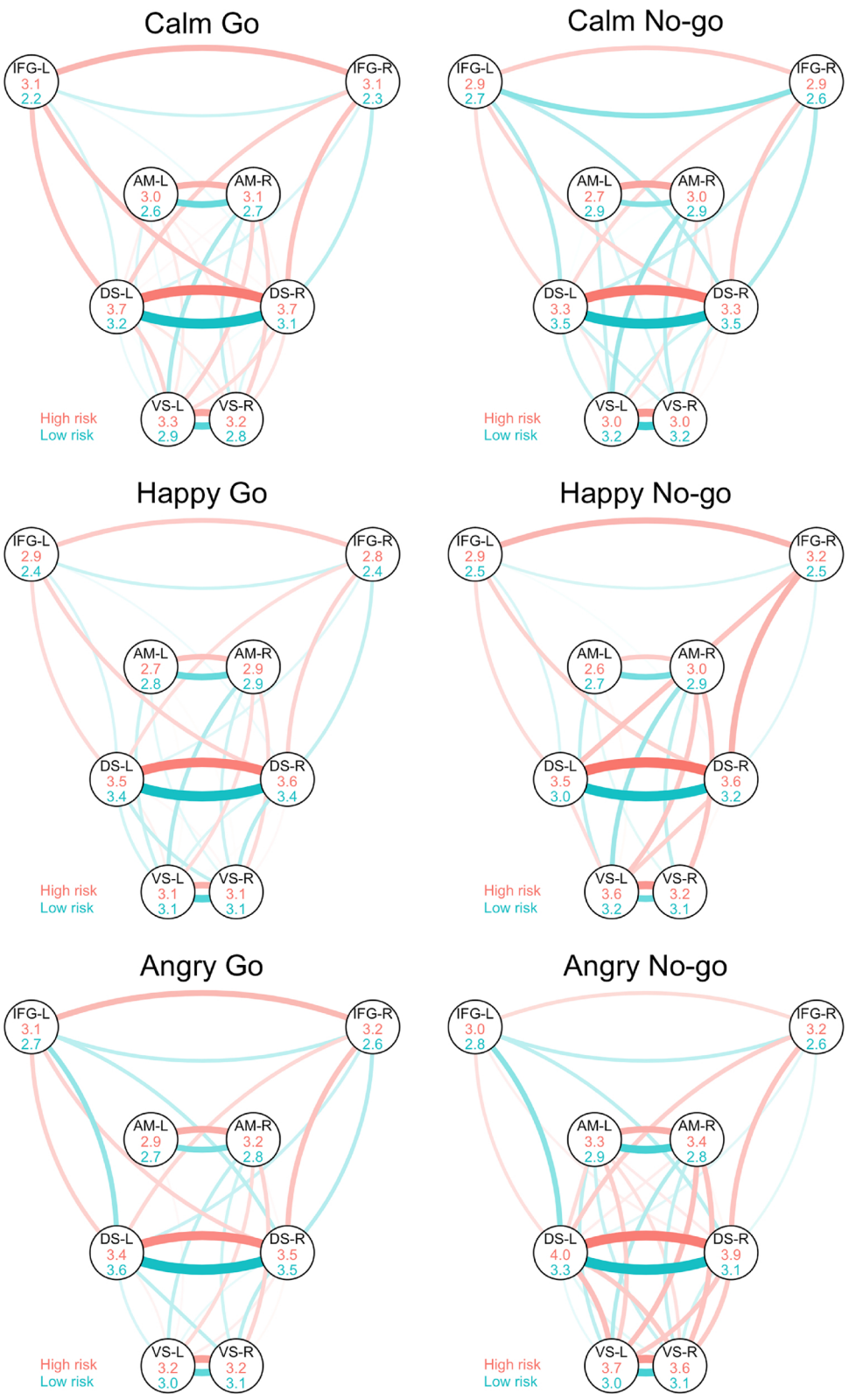

Fig. 7. Functional connectivity networks for he six experimental conditions. Circles indicate the 8 ROIs (left/right inferior frontal gyrus (IFG-L/R), amygdala (AM-L/R), dorsal striatum (DS-L/R), and ventral striatum (VS-L/R). Numbers in the circles indicate the centrality values (red indicates high risk group, blue indicates low risk group), which are also shown in Fig. 6. Lines (red indicates high risk group, blue indicates low risk group) between the ROIs indicate the strength of the correlation between the ROIs. Thicker and less transparent lines indicate higher correlations. (For interpretation of the references to colour in this figure legend, the reader is referred to the web version of this article).

4.2. Neural correlates of emotional cognitive control

Effects of emotional information on cognitive control were also visible at a neural level. Activation in the right IFG was greater for non-target (no-go) than target stimuli, and a similar effect was found at trend level in the right amygdala. These results are in line with previous work, and consistent with proposed models of adolescent inhibitory control. Numerous studies have confirmed the role of the IFG in the suppression of response tendencies in both emotional and neutral contexts, as well as highlighting developmental shifts in this ability, with adolescents often showing particularly strong prefrontal recruitment compared to adults (e.g. Aron et al., 2003; Chikazoe et al., 2009; Luna and Sweeney, 2004). The observed trend-level increased recruitment of the amygdala in our study may be due to the heightened

Table 7
Estimated Marginal Means of the shortest path length values of the dorsal striatum. Standard Errors are in brackets.

Trial Type	Emotion	Risk Group	Dorsal Striatum (left)		Dorsal Striatum (right)	
			Mean	SE	Mean	SE
Go	Angry	High risk	2.238	(0.14)	2.182	(0.14)
		Low risk	2.111	(0.13)	2.159	(0.13)
	Calm	High risk	2.004	(0.14)	2.012	(0.14)
		Low risk	2.333	(0.13)	2.343	(0.13)
	Happy	High risk	2.161	(0.14)	2.123	(0.14)
		Low risk	2.192	(0.13)	2.177	(0.13)
No-go	Angry	High risk	1.852	(0.14)	1.861	(0.14)
		Low risk	2.312	(0.13)	2.357	(0.13)
	Calm	High risk	2.293	(0.14)	2.310	(0.14)
		Low risk	2.176	(0.13)	2.153	(0.13)
	Happy	High risk	2.121	(0.14)	1.977	(0.14)
		Low risk	2.399	(0.13)	2.281	(0.13)

importance of the expressed facial emotions during no-go trials, as the content of the facial expressions (whether calm, happy or angry) then signifies the need for a change in dominant behaviour. This would be in line with the crucial role of the amygdala in the processing of emotional cues (Costafreda et al., 2008; Davis and Whalen, 2001; Ledoux, 2000), as well as signalling the salience and relevance of (social) stimuli (Adolphs, 2010). Scherf et al. (2013) have suggested that this is particularly the case during adolescence, when hormonal changes during puberty result in the amygdala playing a vital role in the evaluation and weighting of specifically social stimuli, resulting in an increased relevance of social signals such as facial emotions.

At an uncorrected threshold of $p < .05$, we also observed an interaction between Emotion and Trial Type in the ventral striatum. Though this effect should be interpreted with caution, it may be explained by the increased salience of emotions during no-go trials. The effect appeared to be driven by a stronger striatal response to happy non-target than happy target faces. The ventral striatum plays an important role in motivated behaviour, especially during the anticipation and attainment of reward (Delgado, 2007; Galvan et al., 2006; Knutson and Greer, 2008), suggesting that the increased relevance of happy faces during non-target trials resulted in greater activation in our sample. Some recent work has also shown striatal activation in response to aversive outcomes, such as negative social feedback (Guyer et al., 2009), or the administration of an aversive liquid (Galvan and McGlennen, 2013) or auditory stimulus (Levita et al., 2009), indicating a general sensitivity of this region to valenced stimuli, not just to reward. We did not observe a difference between target and non-target trials for angry faces. This suggests that the type of stimulus used may be an important, with negative facial expressions not eliciting significant striatal responses. This suggestion is supported by previous work using fearful and happy facial emotions (Dreyfuss et al., 2014; Hare et al., 2008).

4.3. Differences in functional connectivity networks between risk-taking groups

Fronto-striatal circuitry has been identified as critical to goal-directed and motivated behaviour in both adolescents and adults (Balleine et al., 2007; Casey, 2015). Previous work examining the inhibition of approach responses to appetitive stimuli has suggested that the functional organisation of the fronto-striatal network increases during adolescence and into adulthood, and that during adolescence the ventral-dorsal striatal coupling within this network is stronger than during adulthood (Somerville et al., 2011). Other work has shown that viewing emotional stimuli can reduce connectivity in cognitive control networks (Patterson et al., 2016). In this study we used graph-theoretical measures to examine functional connectivity networks. This enabled us to succinctly summarize the properties of the functional networks and identify the influence of brain regions under different conditions of the experiment. As opposed to more traditional methods, where every connection in a network is analysed separately, the graph-theoretical approach thus allows identification of the properties of an entire network and its most important brain regions. By using this method, we were able to establish differences between the risk-taking groups that were not visible when analysing each of the ROIs separately.

Our analyses suggest there are differences between high and low risk-taking adolescents in the recruitment of fronto-striatal networks when regulating behaviour in emotional contexts. As the inhibitory control demands increase within emotional contexts (i.e. happy and angry no-go vs go trials), the centrality of the dorsal striatum increases in the high risk-taking group, and this is accompanied by shorter path lengths within the network. These effects are reversed in the low risk-taking group. Though previous work has often focussed on the role of the ventral striatum during adolescence, our findings suggest that the dorsal striatum may play a central role in emotion regulation during this period. The dorsal striatum is strongly interconnected with motor and higher cortical association areas in frontal and parietal regions, while the ventral striatum shows strong connections with regions involved in emotional processing such as the ventral prefrontal cortex, amygdala and anterior cingulate (Porter et al., 2015). The dorsal striatum is often associated with learning and habit formation (Kimchi et al., 2009), but has also been identified as a convergence point for signals from prefrontal cognitive control regions and the ventral striatum during goal-directed, motivated behaviour (Haber et al., 2006; Haber and Knutson, 2009). Our findings are in line with this model, and suggest that when regulating both positive and negative emotionally salient cues, this role of the dorsal striatum may be of particular importance in those adolescents more prone to risk-taking behaviour. The increased centrality scores in the dorsal striatum were due to greater interconnections with other regions in the high risk-taking group (also reflected by shorter path lengths), and not due to changes in (a small number of) specific connections within the network (as is shown in Fig. 7). Therefore, the increased centrality may reflect greater engagement of fronto-striatal networks from the dorsal striatum when correctly suppressing responses to emotional stimuli. As no differences were observed between the groups in behavioural responses, it seems that the adolescents in the high risk-taking group may require greater coordination within the fronto-striatal network through the dorsal striatum to achieve the same level of performance as low risk-takers.

4.4. Limitations and conclusions

A number of limitations of the present study must be noted. Risk-taking groups were defined based on CCT performance, and not on reports of actual risk-taking behaviours. Previous work has however shown that performance on risk-taking tasks is related to real-world engagement in risk-taking behaviours (Lejuez et al., 2003), as well as demonstrating a positive correlation between self-reported inhibitory control and behavioural measures of inhibition in the presence of emotionally salient stimuli (Shuster and Toplak, 2009). However, further research is needed to confirm these relationships for the behavioural task used in our study. As our sample comprised only adolescents, further work examining children and adults is needed to determine if the observed effects are adolescent-specific. Previous work comparing performance on a variant of the emotional Go-Nogo task in children, adolescents and adults suggests that this may indeed be the case (Somerville et al., 2011). Finally, while not unusual for fMRI research, the size of the risk-taking groups in our sample was relatively small. Though by selecting participants from a larger sample based on their risk-taking behaviour we were able to create more homogeneous groups than would be expected if participants had been recruited from

the general population, thereby increasing the ability to examine the differential effects of high and low levels of risk-taking. Our sample size was largely influenced by the fact that many participants in our longitudinal study had braces, and therefore were not suitable for participation in MRI research. This constraint is important to consider when working with adolescent samples, and oversampling may be required when aiming to select specific groups of participants.

In conclusion, the results of the present study suggest that both appetitive and aversive emotional cues lead to impairments in inhibitory control during adolescence. While no behavioural differences were observed between the risk-taking groups, functional connectivity analyses revealed differences at a neural level. The dorsal striatum was shown to play an essential role within the fronto-striatal network in the high risk-taking group when suppressing responses to emotional cues. These findings offer an initial suggestion that variance in fronto-striatal circuitry may underlie individual differences in risk-taking behaviour, though further research is needed to elucidate this relationship.

Conflict of Interest

None

Acknowledgements

This work was supported by a grant from the National Initiative Brain and Cognition (NIHC 056-34-016 awarded to MH). LK and NL were also funded by an ERC Consolidator Grant (648082 awarded to LK).

Appendix A. Control Region analysis

Processing

To examine the specificity of our ROI and connectivity analyses we performed the analysis using control ROIs. We used the bilateral Occipital Fusiform Gyrus (OFG, Harvard Oxford atlas, with a probability threshold > 50%) and Heschl's gyrus (Harvard Oxford atlas with a probability threshold > 30%) as control regions. These four regions were chosen as we expected no task effects in these regions. Additionally, the control ROIs showed no overlap with our whole-brain contrasts (no-go > go and emotional > calm).

The processing pipeline was the same as in our reported analyses. For the region-of-interest analysis we extracted data using 4 mm spheres from the control ROIs. For the connectivity analysis we used the first eigenvector time-series to estimate beta-series. Functional networks were again created using the first 16 values from the beta-series within a bootstrap framework. We performed a mixed model ANOVA with a random intercept across subjects.

We also used the same strategy to interpret effects. We used a Bonferroni threshold based on 4 regions (alpha = 0.05/4 = 0.0125, alpha < 0.025 for trends) and interpreted bilateral effects at alpha = 0.05 (0.1 for trends).

Results

Results for the ROI activation showed no effects in the left OFG (all p's > .125), right OFG (all p's > .026), and left Heschl's gyrus (all p's > .181). In the right Heschl's gyrus we observed an Emotion by Trial Type trend ($F(2, 160) = 3.886$; $p = .023$).

Results for the centrality measures showed no effects in the left OFG (all p's > .043), right OFG (all p's > .108), and left Heschl's gyrus (all p's > .218). In the right Heschl's gyrus we observed a Risk group by Trial Type trend ($F(1, 160) = 6.035$; $p = .015$).

Appendix B

See Table B1

Table B1
The average connection strength of the left and right dorsal striatum (DS) with the other ROIs in the network for the Emotion, Trial Type and Risk-taking group conditions.

DS	Trial Type	Emotion	Risk Group	Amyg (L)	Amyg (R)	IFG (L)	IFG (R)	VS (L)	VS (R)	DS (R/L)
Left	Go	Angry	High risk	0.30	0.32	0.50	0.48	0.38	0.28	0.79
			Low risk	0.33	0.32	0.55	0.44	0.41	0.47	0.87
		Calm	High risk	0.39	0.36	0.56	0.52	0.50	0.42	0.84
			Low risk	0.29	0.28	0.42	0.41	0.37	0.34	0.87
		Happy	High risk	0.30	0.29	0.48	0.47	0.38	0.36	0.84
			Low risk	0.28	0.31	0.42	0.40	0.43	0.46	0.89
	No-go	Angry	High risk	0.47	0.40	0.45	0.52	0.58	0.53	0.83
			Low risk	0.22	0.18	0.57	0.39	0.38	0.39	0.86
		Calm	High risk	0.26	0.34	0.47	0.48	0.41	0.33	0.84
			Low risk	0.34	0.34	0.49	0.45	0.44	0.44	0.85
		Happy	High risk	0.19	0.20	0.47	0.56	0.46	0.30	0.87
			Low risk	0.17	0.19	0.41	0.29	0.21	0.28	0.86
Right	Go	Angry	High risk	0.25	0.35	0.49	0.57	0.40	0.35	0.79
			Low risk	0.30	0.30	0.47	0.49	0.37	0.47	0.87
		Calm	High risk	0.35	0.36	0.56	0.56	0.47	0.43	0.84
			Low risk	0.23	0.26	0.37	0.47	0.35	0.40	0.87
		Happy	High risk	0.30	0.32	0.51	0.51	0.34	0.36	0.84
			Low risk	0.27	0.32	0.36	0.46	0.41	0.48	0.89
	No-go	Angry	High risk	0.41	0.36	0.39	0.56	0.54	0.54	0.83
			Low risk	0.19	0.19	0.47	0.39	0.33	0.43	0.86
		Calm	High risk	0.24	0.29	0.49	0.53	0.37	0.35	0.84
			Low risk	0.33	0.31	0.48	0.50	0.43	0.44	0.85
		Happy	High risk	0.20	0.23	0.51	0.63	0.51	0.35	0.87
			Low risk	0.08	0.17	0.35	0.40	0.16	0.31	0.86

References

Adolphs, R., 2010. What does the amygdala contribute to social cognition? Ann. N. Y. Acad. Sci. 1191, 42–61.

Allen, J.P., Porter, M.R., McFarland, F.C., Marsh, P., McElhaney, K.B., 2005. The two faces of adolescents' success with peers: adolescent popularity, social adaptation, and deviant behavior. Child Dev. 76 (3), 747–760.

Aron, A.R., Fletcher, P.C., Bullmore, E.T., Sahakian, B.J., Robbins, T.W., 2003. Stop-signal inhibition disrupted by damage to right inferior frontal gyrus in humans. Nat. Neurosci. 6 (2), 115–116. http://dx.doi.org/10.1038/nn1003.

Balleine, B.W., Delgado, M.R., Hikosaka, O., 2007. The role of the dorsal striatum in reward and decision-making. J. Neurosci. 27 (31), 8161–8165. http://dx.doi.org/10.1523/JNEUROSCI.1554-07.2007.

Baumgartner, S.E., Weeda, W.D., van der Heijden, L.L., Huizinga, M., 2014. The relationship between media multitasking and executive function in early adolescents. J. Early Adolesc. 34 (8), 1120–1144. http://dx.doi.org/10.1177/0272431614523133.

Bjork, J.M., Smith, A.R., Chen, G., Hommer, D.W., 2010. Adolescents, adults and rewards: comparing motivational neurocircuitry recruitment using fMRI. PLoS One 5, e11440.

Buelow, M.T., Barnhart, W.R., 2018. Test-retest reliability of common behavioral decision making tasks. Arch. Clin. Neuropsychol. 33, 125–129.

Bullmore, E., Sporns, O., 2009. Complex brain networks: graph theoretical analysis of structural and functional systems. Nat. Rev. Neurosci. 10, 186–198.

Carver, C.S., Harmon-Jones, E., 2009. Anger Is an approach-related affect: evidence and implications. Psychol. Bull. 135 (2), 183–204. http://dx.doi.org/10.1037/a0013965.

Casey, B.J., 2015. Beyond simple models of self-control to circuit-based accounts of adolescent behavior. Annu. Rev. Psychol. 66, 295–319. http://dx.doi.org/10.1146/annurev-psych-010814-015156.

Casey, B.J., Galvan, A., Somerville, L.H., 2016. Beyond simple models of adolescence to an integrated circuit-based account: a commentary. Dev. Cognit. Neurosci. 17, 128–130.

Chein, J., Albert, D., O'Brien, L., Uckert, K., Steinberg, L., 2011. Peers increase adolescent risk taking by enhancing activity in brain's reward circuitry. Dev. Sci. 14, F1–F10.

Chikazoe, J., Jimura, K., Asari, T., Yamashita, K.-i., Morimoto, H., Hirose, S., Konishi, S., et al., 2009. Functional dissociation in right inferior frontal cortex during performance of Go/No-Go task. Cereb. Cortex 19 (1), 146–152. http://dx.doi.org/10.1093/cercor/bhn065.

Cohen-Gilbert, J.E., Thomas, K.M., 2013. Inhibitory control during emotional distraction across adolescence and early adulthood. Child Dev. 84 (6), 1954–1966. http://dx.doi.org/10.1111/cdev.12085.

Costafreda, S.G., Brammer, M.J., David, A.S., Fu, C.H.Y., 2008. Predictors of amygdala activation during the processing of emotional stimuli: a meta-analysis of 385 PET and fMRI studies. Brain Res. Rev. 58 (1), 57–70. http://dx.doi.org/10.1016/j.brainresrev.2007.10.012.

Cousineau, D., 2005. Confidence intervals in within-subject designs: a simpler solution to Loftus and masson's method. Tutorials Quantitat. Methods Psychol. 1 (1), 42–45.

Crone, E.A., Dahl, R.E., 2012. Understanding adolescence as a period of social-affective engagement and goal flexibility. Nat. Rev. Neurosci. 13 (9), 636–650. http://dx.doi.org/10.1038/nrn3313.

Davis, M., Whalen, P.J., 2001. The amygdala: vigilance and emotion. Mol. Psychiatry 6, 13–34.

Delgado, M.R., 2007. Reward-related responses in the human striatum. Ann. N.Y. Acad. Sci. 1104, 70–88. http://dx.doi.org/10.1196/annals.1390.002.

Dreyfuss, M., Caudle, K., Drysdale, A.T., Johnston, N.E., Cohen, A.O., Somerville, L.H., Casey, B.J., et al., 2014. Teens impulsively react rather than retreat from threat. Dev. Neurosci. 36 (3–4), 220–227. http://dx.doi.org/10.1159/000357755.

Eaton, D.K., Kann, L., Kinchen, S., Shanklin, S., Flint, K.H., Hawkins, J., Centers for Disease Control and Prevention (CDC), et al., 2012. Youth risk behavior surveillance – United States, 2011. Morbidity and mortality weekly report. Surveill. Summ. (Wash., D.C.: 2002) 61 (4), 1–162.

Epskamp, S., Cramer, A.O.J., Waldorp, L.J., Schmittmann, V.D., Borsboom, D., 2012. Qgraph: network visualizations of relationships in psychometric data. J. Stat. Softw. 48 (4), 1–18.

Figner, B., Mackinlay, R.J., Wilkening, F., Weber, E.U., 2009. Affective and deliberative processes in risky choice: age differences in risk taking in the Columbia card task. J. Exp. Psychol. Learn. Mem. Cognit. 35 (3), 709–730. http://dx.doi.org/10.1037/A0014983.

Friston, K.J., Rotshtein, P., Geng, J.J., Sterzer, P., Henson, R.N., 2006. A critique of functional localisers. Neuroimage 30 (4), 1077–1087. http://dx.doi.org/10.1016/j.neuroimage.2005.08.012.

Galvan, A., 2013. The teenage brain: sensitivity to rewards. Curr. Dir. Psychol. Sci. 22 (2), 88–93. http://dx.doi.org/10.1177/0963721413480859.

Galvan, A., McGlennen, K.M., 2013. Enhanced striatal sensitivity to aversive reinforcement in adolescents versus adults. J. Cognit. Neurosci. 25 (2), 284–296.

Galvan, A., Hare, T.A., Parra, C.E., Penn, J., Voss, H., Glover, G., Casey, B.J., 2006. Earlier development of the accumbens relative to orbitofrontal cortex might underlie risk-taking behavior in adolescents. J. Neurosci. 26 (25), 6885–6892. http://dx.doi.org/10.1523/Jneurosci.1062-06.2006.

Geier, C.F., 2013. Adolescent cognitive control and reward processing: implications for risk taking and substance use. Horm. Behav. 64 (2), 333–342. http://dx.doi.org/10.1016/j.yhbeh.2013.02.008.

Geier, C.F., Terwilliger, R., Teslovich, T., Velanova, K., Luna, B., 2010. Immaturities in reward processing and its influence on inhibitory control in adolescence. Cereb. Cortex 20 (7), 1613–1629. http://dx.doi.org/10.1093/cercor/bhp225.

Grose-Fifer, J., Rodrigues, A., Hoover, S., Zottoli, T., 2013. Attentional capture by emotional faces in adolescence. Adv. Cognit. Psychol. 9 (2), 81–91. http://dx.doi.org/10.2478/v10053-008-0134-9.

Guyer, A.E., Monk, C.S., McClure-Tone, E.B., Nelson, E.E., Roberson-Nay, R., Adler, A.D., Ernst, M., et al., 2008. A developmental examination of amygdala response to facial expressions. J. Cognit. Neurosci. 20, 1565–1582.

Guyer, A.E., McClure-Tone, E.B., Shiffrin, N.D., Pine, D.S., Nelson, E.E., 2009. Probing the neural correlates of anticipated peer evaluation in adolescence. Child Dev. 80 (4), 1000–1015.

Haber, S.N., Knutson, B., 2009. The reward circuitry: linking primate anatomy and human imaging. Neuropsychopharmacology 1, 1–23.

Haber, S.N., Kim, K.S., Mailly, P., Calzavara, R., 2006. Reward-related cortical outputs define a large striatal region in primates that interface with associative cortical connections, providing a substrate for incentive-based learning. J. Neurosci. 26, 8368–8376.

Hare, T.A., Casey, B.J., 2005. The neurobiology and development of cognitive and affective control. Cognit. Brain Behav. IX (3), 273–286.

Hare, T.A., Tottenham, N., Galvan, A., Voss, H.U., Glover, G.H., Casey, B.J., 2008. Biological substrates of emotional reactivity and regulation in adolescence during an emotional go-nogo task. Biol. Psychiatry 63 (10), 927–934.

Harmon-Jones, E., Allen, J.J.B., 1998. Anger and frontal brain activity: EEG asymmetry consistent with approach motivation despite negative affective valence. J. Pers. Soc. Psychol. 74 (5), 1310–1316. http://dx.doi.org/10.1037//0022-3514.74.5.1310.

Heller, A.S., Cohen, A.O., Dreyfuss, M.F.W., Casey, B.J., 2016. Changes in cortico-subcortical and subcortico-subcortical connectivity impact cognitive control to emotional cues across development. Soc. Cogn. Affect. Neurosci. 1910–1918. http://dx.doi.org/10.1093/scan/nsw097.

Herba, C., Phillips, M., 2004. Annotation: development of facial expression recognition from childhood to adolescence: behavioural and neurological perspectives. J. Child Psychol. Psychiatry 45 (7), 1185–1198. http://dx.doi.org/10.1111/J.1469-7610.2004.00316.X.

Humphreys, K.L., Lee, S.S., Tottenham, N., 2013. Not all risk taking behavior is bad: associative sensitivity predicts learning during risk taking among high sensation seekers. Pers. Individ. Differ. 54 (6), 709–715. http://dx.doi.org/10.1016/j.paid.2012.11.031.

Jenkinson, M., Smith, S., 2001. A global optimisation method for robust affine registration of brain images. Med. Image Anal. 5 (2), 143–156. http://dx.doi.org/10.1016/S1361-8415(01)00036-6.

Jenkinson, M., Bannister, P., Brady, M., Smith, S., 2002. Improved optimization for the robust and accurate linear registration and motion correction of brain images. Neuroimage 17 (2), 825–841. http://dx.doi.org/10.1006/nimg.2002.1132.

Jenkinson, M., Beckmann, C.F., Behrens, T.E., Woolrich, M.W., Smith, S.M., 2012. Fsl. Neuroimage 62 (2), 782–790. http://dx.doi.org/10.1016/j.neuroimage.2011.09.015.

Kimchi, E.Y., Torregrossa, M.M., Taylor, J.R., Laubach, M., 2009. Neuroanl correlates of instrumental learning in the dorsal striatum. J. Neurophysiol. 102, 475–489.

Knutson, B., Greer, S.M., 2008. Anticipatory affect: neural correlates and consequences for choice. Philos. Trans. R. Soc. Lond. B Biol. Sci. 363, 3771–3786.

Ledoux, J.E., 2000. Emotion circuits in the brain. Annu. Rev. Neurosci. 23, 155–184. http://dx.doi.org/10.1146/annurev.neuro.23.1.155.

Lejuez, C.W., Aklin, W.M., Zvolensky, M.J., Pedulla, C.M., 2003. Evaluation of the balloon analogue risk task (BART) as a predictor of adolescent real-world risk-taking behaviours. J. Adolesc. 26, 475–479. http://dx.doi.org/10.1016/S0140-1971(03)00036-8.

Levita, L., Hare, T.A., Voss, H.U., Glover, G.H., Ballon, D.J., Casey, B.J., 2009. The bivalent side of the nucleus accumbens. NeuroImage 44 (3), 1178–1187. http://dx.doi.org/10.1016/j.neuroimage.2008.09.039.

Luna, B., Sweeney, J.A., 2004. The emergence of collaborative brain function – fMRI studies of the development of response inhibition. Adolesc. Brain Dev.: Vulnerabilities Oppor. 1021, 296–309. http://dx.doi.org/10.1196/annals.1308.035.

Mills, K.L., Goddings, A., Clasen, L.S., Giedd, J.N., Blakemore, S.J., 2014. The developmental mismatch in structural brain maturation during adolescence. Dev. Neurosci. 36, 147–160.

Mumford, J.A., Turner, B.O., Ashby, F.G., Poldrack, R.A., 2012. Deconvolving BOLD activation in event-related designs for multivoxel pattern analysis. Neuroimage 59 (3), 2636–2643. http://dx.doi.org/10.1016/j.neuroimage.2011.08.076.

Nelson, E.E., Jarcho, J.M., Guyer, A.E., 2016. Social re-orientation and brain development: an expanded and updated view. Dev. Cognit. Neurosci. 17, 118–127.

Opsahl, T., Agneessens, F., Skvoretz, J., 2010. Node centrality in weighted networks: generalizing degree and shortest paths. Soc. Netw. 32, 245–251.

Padmanabhan, A., Geier, C.F., Ordaz, S.J., Teslovich, T., Luna, B., 2011. Developmental changes in brain function underlying the influence of reward processing on inhibitory control. Dev. Cognit. Neurosci. 1 (4), 517–529. http://dx.doi.org/10.1016/j.dcn.2011.06.004.

Patterson, T.K., Lenartowicz, A., Berkman, E.T., Ji, D., Poldrack, R.A., Knowlton, B.J., 2016. Putting the brakes on the brakes: negative emotion disrupts cognitive control network functioing and alters subsequent stopping ability. Exp. Brain Res. 234, 3107–3118. http://dx.doi.org/10.1007/s00221-016-4709-2.

Penolazzi, B., Gremigni, P., Russo, P.M., 2012. Impulsivity and reward-sensitivity differentially influence affective and deliberative risky decision making. Pers. Individ. Differ. 53, 655–659.

Pfeifer, J.H., Allen, N.B., 2012. Arrested development? Reconsidering dual-systems models of brain function in adolescence and disorders. Trends Cognit. Sci. 16, 322–329.

Pfeifer, J.H., Allen, N.B., 2016. The audacity of specificity: moving adolescent developmental neuroscience towards more powerful scientific paradigms and translatable models. Dev. Cognit. Neurosci. 17, 131–137.

Poldrack, R.A., Mumford, J.A., Nichols, T.E., 2011. Handbook of Functional MRI Analysis. Cambridge University Press.
Porter, J.N., Roy, A.K., Benson, B., Carlisi, C., Collins, P.F., Leibenluft, E., Ernst, M., et al., 2015. Age-related changes in the instrinsic functional connectivity of the human ventral vs. dorsal striatum from childhood to middle age. Dev. Cognit. Neurosci. 11, 83–95.
Rubinov, M., Sporns, O., 2010. Complex network measures of brain connectivity: uses and interpretations. Neuroimage 52, 1059–1069.
Scherf, K.S., Smyth, J.M., Delgado, M.R., 2013. The amygdala: an agent of change in adolescent neural networks. Horm. Behav. 64, 298–313.
Schulman, E.P., Smith, A.R., Silva, K., Icenogle, G., Duell, N., Chein, J., Steinberg, L., 2016. The dual systems model: review, reappraisal, and reaffirmation. Dev. Cognit. Neurosci. 17, 103–117.
Schultz, K.P., Fan, J., Magidina, O., Marks, D.J., Hahn, B., Halpern, J.M., 2007. Does the emotional go/no-go task really measure behavioral inhibition? Convergence with measures on a non-emotional analog. Arch. Clin. Neuropsychol. 22, 151–160.
Shuster, J., Toplak, M.E., 2009. Executive and motivational inhibition: associations with self-report measures related to inhibition. Conscious. Cognit. 18 (2), 471–480. http://dx.doi.org/10.1016/j.concog.2009.01.004.
Silva, K., Shulman, E.P., Chein, J., Steinberg, L., 2016. Peers increase late adolescents'exploratory behaviour and sensitivity to positive and negative feedback. J. Adolesc. 26, 696–705.
Smith, S.M., 2002. Fast robust automated brain extraction. Hum. Brain. Mapp. 17 (3), 143–155. http://dx.doi.org/10.1002/hbm.10062.
Somerville, L.H., Hare, T., Casey, B.J., 2011. Frontostriatal maturation predicts cognitive control failure to appetitive cues in adolescents. J. Cognit. Neurosci. 23 (9), 2123–2134.
Sporns, O., Zwi, J.D., 2004. The small world of the cerebral cortex. Neuroinformatics 2, 145–162.
Tottenham, N., Tanaka, J.W., Leon, A.C., McCarry, T., Nurse, M., Hare, T.A., Nelson, C., et al., 2009. The NimStim set of facial expressions: judgments from untrained research participants. Psychiatry Res. 168 (3), 242–249. http://dx.doi.org/10.1016/J.Psychres.2008.05.006.
Turner, B.O., Mumford, J.A., Poldrack, R.A., Ashby, F.G., 2012. Spatiotemporal activity estimation for multivoxel pattern analysis with rapid event-related designs. Neuroimage 62 (3), 1429–1438. http://dx.doi.org/10.1016/j.neuroimage.2012.05.057.
Urben, S., Van der Linden, M., Barisnikov, K., 2012. Emotional modulation of the ability to inhibit a prepotent response during childhood. Dev. Neuropsychol. 37 (8), 668–681. http://dx.doi.org/10.1080/87565641.2012.675378.
van Batenburg-Eddes, T., Lee, N.C., Weeda, W.D., Krabbendam, L., Huizinga, M., 2014. The potential adverse effect of energy drinks on executive functions in early adolescence. Front. Psychol. 5 Artn 45710.3389/Fpsyg.2014.00457.
Vink, M., Derks, J.M., Hoogendam, J.M., Hillegers, M., Kahn, R.S., 2014. Functional differences in emotion processing during adolescence and early adulthood. Neuroimage 91, 70–76.
Weber, E.U., Johnson, E.J., 2009. Mindful judgment and decision making. Annu. Rev. Psychol. 60, 53–85.
Worsley, K.J., 2001. Statistical analysis of activation images. In: Jezzard, P., Matthews, P.M., Smith, S.M. (Eds.), Functional MRI: An Introduction to Methods. Oxford University Press, Oxford.